Phagocytosis is coupled to the formation of phagosome-associated podosomes and a transient disruption of podosomes in human macrophages

Margot Tertrais, Claire Bigot, Emmanuel Martin, Renaud Poincloux, Arnaud Labrousse, Isabelle Maridonneau-Parini

▶ **To cite this version:**

Margot Tertrais, Claire Bigot, Emmanuel Martin, Renaud Poincloux, Arnaud Labrousse, et al.. Phagocytosis is coupled to the formation of phagosome-associated podosomes and a transient disruption of podosomes in human macrophages. European Journal of Cell Biology, 2021, 100 (4), pp.151161. 10.1016/j.ejcb.2021.151161 . hal-04731950

HAL Id: hal-04731950

https://ut3-toulouseinp.hal.science/hal-04731950v1

Submitted on 11 Oct 2024

HAL is a multi-disciplinary open access archive for the deposit and dissemination of scientific research documents, whether they are published or not. The documents may come from teaching and research institutions in France or abroad, or from public or private research centers.

L'archive ouverte pluridisciplinaire **HAL**, est destinée au dépôt et à la diffusion de documents scientifiques de niveau recherche, publiés ou non, émanant des établissements d'enseignement et de recherche français ou étrangers, des laboratoires publics ou privés.

Distributed under a Creative Commons Attribution - NonCommercial - NoDerivatives 4.0 International License

European Journal of Cell Biology 100 (2021) 151161

Contents lists available at ScienceDirect

European Journal of Cell Biology

journal homepage: www.elsevier.com/locate/ejcb

Phagocytosis is coupled to the formation of phagosome-associated podosomes and a transient disruption of podosomes in human macrophages

Margot Tertrais [a,1], Claire Bigot [a,1], Emmanuel Martin [b], Renaud Poincloux [a], Arnaud Labrousse [a], Isabelle Maridonneau-Parini [a,*]

[a] Institut de Pharmacologie et Biologie Structurale, IPBS, Université de Toulouse, CNRS, UPS, Toulouse, France
[b] MCD, Centre de Biologie Intégrative (CBI), Université de Toulouse, CNRS, UPS, Toulouse, France

ARTICLE INFO

Keywords:
Podosome
Phagocytosis
Macrophage
Phagolysosome

ABSTRACT

Phagocytosis consists in ingestion and digestion of large particles, a process strictly dependent on actin re-organization. Using synchronized phagocytosis of IgG-coated latex beads (IgG-LB), zymosan or serum opsonized-zymosan, we report the formation of actin structures on both phagocytic cups and closed phagosomes in human macrophages. Their lifespan, size, protein composition and organization are similar to podosomes. Thus, we called these actin structures phagosome-associated podosomes (PAPs). Concomitantly to the formation of PAPs, a transient disruption of podosomes occurred at the ventral face of macrophages. Similarly to podosomes, which are targeted by vesicles containing proteases, the presence of PAPs correlated with the maturation of phagosomes into phagolysosomes. The ingestion of LB without IgG did not trigger PAPs formation, did not lead to podosome disruption and maturation to phagolysosomes, suggesting that these events are linked together. Although similar to podosomes, we found that PAPs differed by being resistant to the Arp2/3 inhibitor CK666. Thus, we describe a podosome subtype which forms on phagosomes where it probably serves several tasks of this multifunctional structure.

1. Introduction

Macrophages are immune cells that are involved in both innate and adaptative immune responses (Jakubzick et al., 2017). They migrate to reach infectious sites and ingest microorganisms, debris and foreign bodies, a process called phagocytosis (Jaumouille and Grinstein, 2016; Uribe-Querol and Rosales, 2020). Both migration and phagocytosis rely on a strong and coordinated re-organization of the actin cytoskeleton. Phagocytosis is the specialized capacity of a subpopulation of immune cells called phagocytes to ingest particles larger than 0.5 μm. Despite the discovery of phagocytosis at the end of the 19th century, many aspects of this process remain unclear. During phagocytosis, actin polymerization is responsible for engulfment of particles and phagosome maturation (Freeman and Grinstein, 2014; Gray and Botelho, 2017). However, the dynamics of actin polymerization at phagosomes is regulated differently when FcγR for IgG or CR3 receptors are engaged (Allen and Aderem, 1996; Caron and Hall, 1998; Jaumouille and Waterman, 2020; Rotty et al., 2017).

During the first steps of phagocytosis, actin filaments organize as a dense meshwork underlying the plasma membrane in a structure called the phagocytic cup. Following the formation of this cup, actin re-organizes progressively all around the particle until closure of the phagosome membrane. Then, the phagosome traffics along microtubules and sequentially fuses with endosomes and lysosomes to form phagolysosomes (Uribe-Querol and Rosales, 2020). Along this maturation process, the phagosome progressively loses its F-actin coat. The abundance of actin around the phagosome determines its capacity to fuse with lysosomes. The presence of a dense actin meshwork inhibits the fusion of phagosomes with lysosomes (Jahraus et al., 2001; Liebl and Griffiths, 2009), whereas a less abundant organization of actin filaments at the phagosome membrane can serve as tracks for lysosomes to move forward phagosomes (Anes et al., 2003; Jahraus et al., 2001; Kjeken et al., 2004). Moreover, flashes of actin have been described on a small proportion of mature phagosomes in RAW 264.7 macrophages that

Abbreviations: PAP, phagosome-associated podosome; LB, latex beads; IgG-LB, IgG-coated latex beads; Z, zymosan; OZ, serum-opsonized zymosan.

* Corresponding author at: Institut de Pharmacologie et Biologie Structurale, CNRS UMR5089, 205 route de Narbonne, 31400 Toulouse, France.
E-mail address: maridono@ipbs.fr (I. Maridonneau-Parini).

[1] Co-first authors.

https://doi.org/10.1016/j.ejcb.2021.151161
Received 16 October 2020; Received in revised form 8 March 2021; Accepted 29 March 2021
Available online 31 March 2021
0171-9335/© 2021 The Author(s). Published by Elsevier GmbH. This is an open access article under the CC BY-NC-ND license (http://creativecommons.org/licenses/by-nc-nd/4.0/).

ingest IgG-coated particles, as well as in non-phagocytic cells infected by *Listeria monocytogenes* (Liebl and Griffiths, 2009; Yam and Theriot, 2004). More recently, flashes have been shown to form on the phagosome surface when phagocytosis is mediated by complement receptors but not by Fc receptors and they are more abundant when particle stiffness decreases (Poirier et al., 2020). Dynamic analysis of these flashes indicated that actin filaments follow several assembly/disassembly cycles, a phenomenon that lasts the first hour of the phagocytic process and that is Arp2/3-dependent. Despite some contradictory results, the proposed function of actin flashes is to contract phagosomes and improve the degradation of the phagosome content (Liebl and Griffiths, 2009; Poirier et al., 2020).

In addition to these actin structures present on closed phagosomes, podosome-like structures have also been observed at phagocytic cups (Allen and Aderem, 1996; Labrousse et al., 2011; Ostrowski et al., 2019). Podosomes, constitutively form in macrophages, dendritic cells and osteoclasts, and participate in cell adhesion, proteolysis of the extracellular matrix and mechanosensing of the cellular environment. They comprise a dense core of F-actin, surrounded at its basis by a ring of adhesion complexes linked to the actin cytoskeleton (van den Dries et al., 2019). In dense and non-penetrable environments, podosomes are involved in opening paths that allow the migration of macrophages (Maridonneau-Parini, 2014). The podosome-like structures described at phagocytic cups are similar to podosomes in term of composition and architecture but can be distinguished by their lifespan and distinct regulators of their formation (Allen and Aderem, 1996; Labrousse et al., 2011; Ostrowski et al., 2019). The podosome-like structures found on early phagosomes were proposed to mediate particle internalization (Allen and Aderem, 1996) and to perform a mechanical sealing of the phagosome membrane with the ingested particle (Ostrowski et al., 2019). This mechanical function is reminiscent of the force that is required to zip the phagosome membrane around particles and to detect the rigidity of the extracellular environment by podosomes (Jaumouille and Grinstein, 2016; Labernadie et al., 2014; Mylvaganam et al., 2018). Podosomes are targeted by late endosomes/lysosomes that deliver proteases, including MT1-MMP, in their close vicinity (Cougoule et al., 2005, 2010; Jeannot and Besson, 2020; Marchesin et al., 2015; Monteiro et al., 2013; Wiesner et al., 2010). Phagosomes also fuse with endosomes and lysosomes, a process known as phagosome maturation, the resulting phagolysosome offers a specialized acidic and hydrolytic milieu dedicated to degradation of the engulfed particle. It is therefore tempting to hypothesize that podosome-like structures are not only involved in the early stages of phagocytosis but also play a role all along phagosome maturation. However, it is still unknown whether podosome-like structures are present after phagosome closure.

We therefore examined whether podosome-like structures i) are present on closed phagosomes, ii) form around any particles regardless of the phagocytic pathway, iii) correlate with phagolysosome formation, and iv) impact the formation of podosomes at the ventral membrane of macrophages.

2. Materials and methods

2.1. Products and antibodies

Zymosan A (Z4250) was provided by Sigma-Aldrich. Latex microbeads (Fluoresbrite Yellow Green Microspheres, 17155-2) was from Polyscience. CK-666 (ab141231) was purchased from Abcam. Phalloidin-546 and -647, secondary antibodies donkey anti-mouse (Alexa Fluor 647) and goat anti-mouse (Alexa Fluor 647) were purchased from Fischer Scientific and all used at a 1:200 dilution. Mouse monoclonal antibodies anti-Cortactin (1:100, p80/85, clone 4F11), and rabbit anti-ovalbumin (1:10, ab1225) were from Millipore. Anti-vinculin (1:100, V9131, clone HVIN-1) antibodies and goat anti-rabbit TRITC were purchased from Sigma. Paxillin antibodies (1:100, P13520) was from BD Transduction Laboratories and anti-LAMP1 (1:100, clone H4A3) from Santa Cruz. Rab 5 antibodies (1:100, clone 2E8B11) were from ThermoFischer. CD18 antibodies (1:100, clone MHM23) from Dako. Human MCSF (130−096-489) was purchased from Miltenyi (France). Fluorescein isothiocyanate (F1906) was provided by Molecular Probes.

2.2. Cells

Human monocytes were isolated from the blood of healthy donors (buffy coats obtained from Etablissement Français du Sang) and differentiated into human monocyte–derived macrophages (hMDMs) as previously described (Van Goethem et al., 2010). After cell sorting with CD14-magnetic beads, monocytes were differentiated in RPMI culture medium with 10% FCS (Fisher Scientific, France) containing 20 ng/mL of human M-CSF for 7–8 days before their use. The culture medium was usually renewed on the third or fourth day. In experiments with CK666, macrophages were pre-incubated for 15 min with either the drug solubilized in DMSO or vehicle.

2.3. Phagocytosis assays

Zymosan A (Z, 10 mg) was placed overnight at 4 °C in rotation with FITC (0.5 mg/mL) in 1 mL of bicarbonate reaction buffer (0.25 M pH 9) then washed with PBS (Fisher Scientific). For opsonisation, FITC-labelled zymosan was incubated at 37 °C under agitation with human serum (H4522, Sigma-Aldrich) at 37 °C for 30 min then washed with PBS.

Latex beads (LB, Fluoresbrite yellow green, Polyscience, diameter : 3 μm) were coated with ovalbumin (1 mg/mL in PBS) for 1 h at room temperature and washed with PBS containing BSA (10 mg/mL, 115004696, Fisher Scientific). To obtain IgG-opsonized latex beads, ovalbumin-coated beads were then incubated with anti-ovalbumin antibodies for a hour (1:10, room temperature) and washed 3 times.

Particles were added to macrophages at several multiplicity of infection (MOI) to obtain equivalent rates of phagocytosis. Z and LB were used at MOI 30:1; IgG-LB and OZ at MOI 10:1 with macrophages plated on coverslips. Phagocytosis was synchronized with a centrifugation at 170 *g* for 5 min. Unbound beads were washed off with culture medium and cells were then incubated at 37 °C for the indicated time points. In some experiments, to chelate divalent cations, EDTA (5 mM) was added to the medium concomitantly to IgG-LB and the phagocytosis assay was carried-out for 5 min.

2.4. Immunofluorescence

After cell fixation for 30 min at RT with 3.7 % paraformaldehyde in PBS containing 15 mM sucrose, unreacted aldehyde functions were quenched with 50 mM NH_4Cl in PBS for 5 min at RT as previously described (Labernadie et al., 2010). Cells were then washed and permeabilized with 0.1 % Triton X100 in PBS for 10 min at RT before being saturated with 5% BSA in PBS for 30 min at RT. Cells were then stained with primary antibodies in the presence of 5% BSA (PBS/BSA) for 30 min at RT, washed three times in PBS and incubated in the dark with a mixture of secondary antibodies and fluorescent phalloidin (546 or 647, to detect F-actin) for 30 min at RT. Samples were then mounted with the fluorescent mounting medium from DAKO.

To determine whether green latex beads were internalized or not, cells challenged with IgG-coated LB were fixed and subjected to TRITC-conjugated goat anti-rabbit secondary antibodies (1:150 dilution) without cell permeabilization. When cells were challenged with LB, they were fixed and not permeabilized, subjected to anti-ovalbumin antibodies and revealed by TRITC secondary antibodies. Thus, yellow beads (green + red) are those remained outside while green beads were inside phagosomes. This approach also attested that phagosomes are sealed when they contain green beads.

2.5. Microscopy and image analysis

Immunofluorescent samples were observed using a PL Fluotar 40x/NA 1.0–0.5 oil immersion objective on a Leitz DM-RB microscope, equipped with a CoolSnap HQ CCD camera (Roper Scientific) and the Metaview sofware (Roper Scientific).

When indicated, super-resolution images were obtained using a LSM880 confocal microscope equipped with a Fast Airyscan module (Carl Zeiss) and is with and a Plan-Apochromat 40x/NA 1.3 oil DIC UV-IR M27 objective. Z-stack were acquired using the Super Resolution mode (Airyscan), set with a pixel size of 0.053 µm/pixel and a *z*-step of 0.249 µm. Airyscan Z-stacks were processed in ZEN software using the automatic strength (6 by default) and the 3D method.

Podosomes in F-actin stained cells were quantified with Fiji software. Briefly, podosome cores were detected using the "Find Maxima" function of the software. To calculate the number of cells with podosomes, cells with less than 10 podosomes were considered as podosome-free. Podosome density was calculated for each cell by dividing the podosome number by the cell surface (measured by manual cell delimitation).

Intensity profiles of vinculin, paxillin, talin, cortactin, CD18 and F-actin were measured on the phagosome surface in the area of PAPs by using the « Plot profile » function of Image J. The maximal fluorescence intensity of each profile was normalized to 100. Mean values were calculated on PlotTwist application (Goedhart, 2020). The height of PAPs was determined by the full width at half maximum of the intensity peak of F-actin from Airyscan acquisition.

2.6. Live cell imaging

Human macrophages were transduced with Lifeact-mCherry expressing lentiviruses as previously described (Van Goethem et al., 2011) after 4 days of differentiation. Two days later, cells were harvested and seeded in Lab-tek™ glass based chambers and kept in a humidified atmosphere at 37 °C and 5% CO_2 for at least 18 h. Live cell imaging was performed using an Olympus IX81 microscope equipped with a 100X oil immersion objective, a Yokogawa CSU22 confocal unit and an Andor iXon 888-BVEM–CCD back illuminated camera. Stacks of 11 sections spaced by 0.7 µm were acquired every 30 s using Andor IQ 1.9 Software.

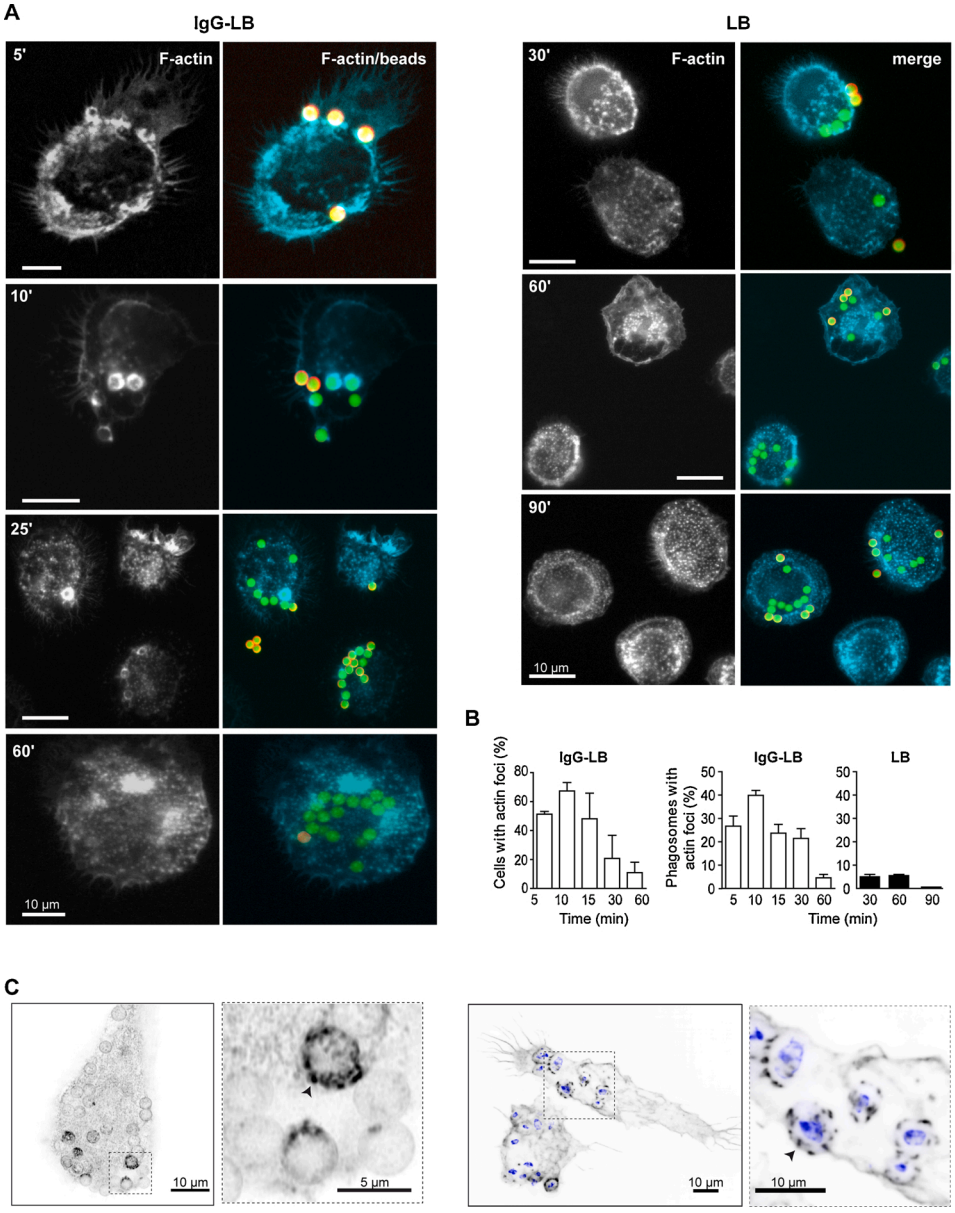

Fig. 1. F-actin structures are present at the membrane of nascent and closed phagosomes. Images of fluorescence microscopy (A). Human macrophages cultured on glass coverslips were exposed to fluorescent latex beads (green) coated with IgG (IgG-LB : MOI 10:1) or not (LB : MOI 30:1). The beads were centrifuged to synchronize phagocytosis and the experiments were carried out for the indicated times. F-actin (cyan) structures form on phagocytic cups (5 min) and closed phagosomes containing IgG-LB, they did not form on phagosomes containing LB. Beads inside sealed phagosomes are green, beads outside were stained in red (they appear yellow in merge images). Scale bars: 10 µm. (B) Quantification of the percentage of cells with actin structures on phagosomes (left) and the percentage of phagosomes containing IgG-LB (middle) or LB (right) with actin structures. Results from at least 25 cells per time point from 2 to 5 donors are expressed as mean +/- SD. (C) Macrophages containing IgG-LB were fixed at 10 min, those containing OZ, fixed at 15 min, and stained for F-actin and analyzed by Airyscan super-resolution microscopy. In the cropped images, arrowheads point to F-actin foci on phagosomes. (For interpretation of the references to colour in this figure legend, the reader is referred to the web version of this article).

2.7. Statistics

Statistical analyses were performed using Prism 5 (GraphPad). Statistical comparison of the data was performed using one-way Anova followed by Dunnett's comparison test or by Kruskal-Wallis test, followed by Dunn's multiple comparisons test for not normally distributed data. For EDTA, statistical comparison was performed using paired *t*-test followed by Wilcoxon test. In the figures, statistical significance is indicated as follows: * $p < 0.05$; ** $p < 0.01$ and *** $p < 0.001$.

3. Results

3.1. F-actin structures form on phagocytic cups and closed phagosomes

To determine whether F-actin structures are present on closed phagosomes, experiments of synchronized phagocytosis were performed with fluorescent 3 μm-large latex beads that were coated with IgG (IgG-LB) or not (LB). Phagocytosis of IgG-LB and LB was carried out with 10 and 30 particles/cell, respectively, in order to obtain similar phagocytic rates (Suppl. Fig. 1A). Next, as shown in Fig. 1, beads inside sealed phagosomes (green) were distinguished from beads that were not internalized (yellow, see Materials and Methods). At 5 min of phagocytosis of IgG-LB, we noticed that F-actin structures were present on phagocytic cups (see phagocytic cups containing beads with a yellow/red apex attesting that phagosomes are unclosed) and, at later time points, they were also observed on closed phagosomes (Fig. 1A). The percentage of cells with F-actin foci at phagosomes was maximal at 10 min and then decreased until 60 min (Fig. 1B). The percentage of phagosomes with actin structures was 25 % at 5 min; it peaked at 10 min at about 40 % and went back to almost zero at 60 min. Contrasting with

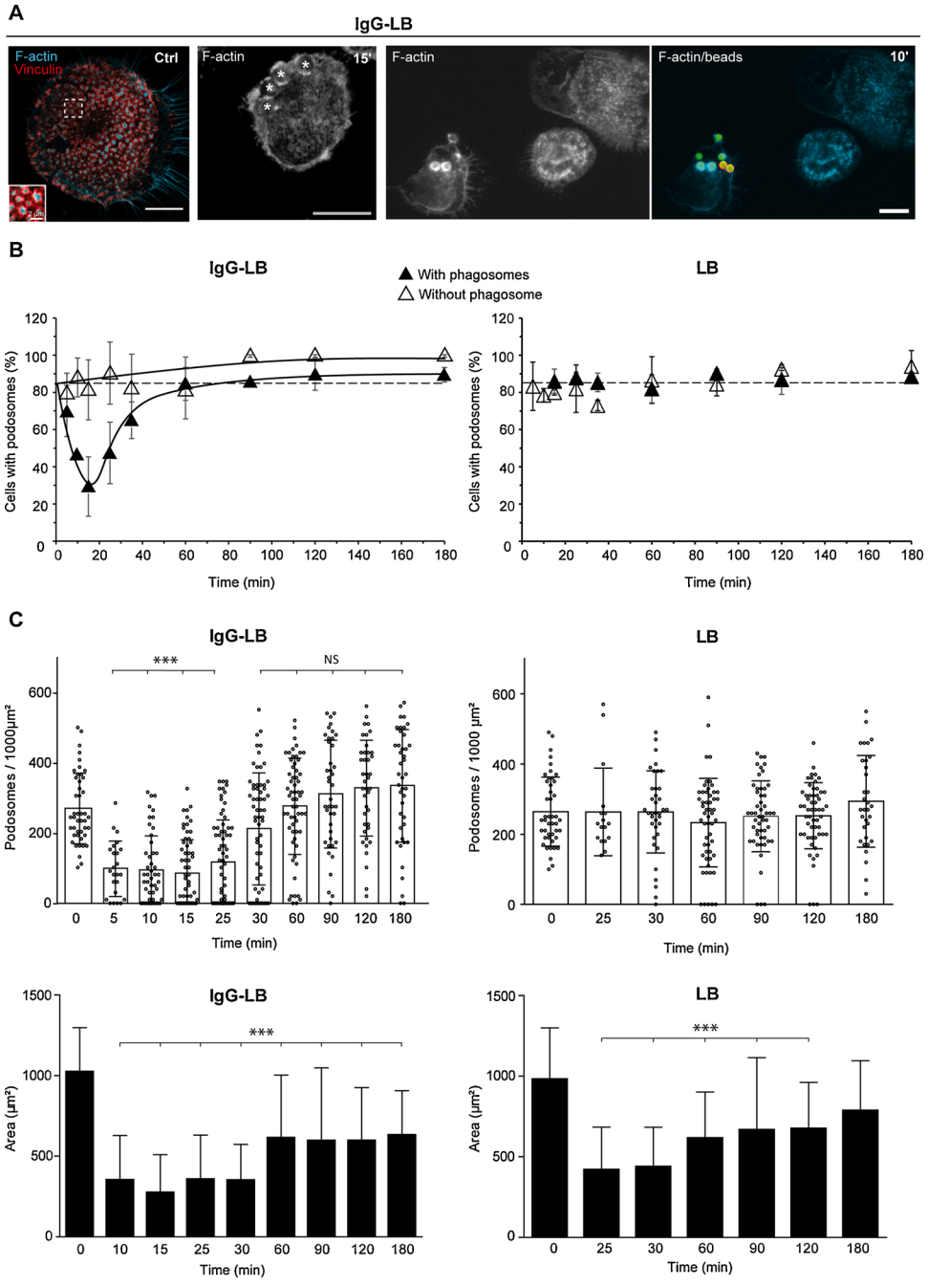

Fig. 2. Phagocytosis of IgG-IgG-LB leads to transient disruption of podosomes. Human macrophages cultured on glass coverslips were exposed to IgG-LB (MOI 10:1) or LB (MOI 30:1). The beads were centrifuged to synchronize phagocytosis and the experiments were carried out for the indicated times (5 to 180 min). Images of fluorescence microscopy (A): the left image shows podosomes in a control cell not exposed to beads, the neighbor image shows podosome disruption at 15 min in a cell with phagosomes (materialized by stars); the two images on the right show that podosomes remain in cells that do not ingest beads while they disappear in the neighbor cells with phagosomes. Beads inside cells are green, beads outside are yellow, F-actin is cyan. Scale bars: 10 μm. (B) The percentage of cells with podosomes were quantified in cells containing phagosomes and in neighbor cells without phagosomes. The dash line is the percentage of macrophages with podosomes in control cells that were not exposed to beads. Results are expressed as mean +/- SD of at least 50 cells/time point from 3 donors ; and analyzed with Kruskal-Wallis test, followed by Dunn's multiple comparisons test. (C) The podosome density was quantified by measuring the cell area (lower panels) and counting the number of podosomes. Results are expressed as mean +/- SD of at least 20 cells/time point from 3 donors, and analyzed using a Kruskal-Wallis test, followed by Dunn's multiple comparisons test. (For interpretation of the references to colour in this figure legend, the reader is referred to the web version of this article).

these results, phagosomes containing LB only occasionally presented F-actin at their surface (Fig. 1B). Next, the actin structures were examined by super-resolution microscopy on closed phagosomes. They looked similar in size and distribution when either IgG-LB or serum-opsonized zymosan (OZ) were used (Fig. 1C, Video 1). Thus, in human macrophages, F-actin structures formed at the surface of phagocytic cups and closed phagosomes containing IgG-LB, OZ but not LB.

3.2. *Podosomes are transiently disrupted concomitantly to the formation of actin structures on phagosomes*

While we were imaging actin structures on phagosomes at different time points, we noticed that podosomes at the ventral face of macrophages disappeared (Fig. 1A). We therefore quantified it.

As observed in Fig. 1A, at early time points of the phagocytosis process (5 and 10 min), podosomes disappeared and they re-appeared later on (30 and 60 min). In Fig. 2A, the superresolution images on the left show podosomes in a macrophage devoid of phagosomes to compare with a macrophage containing phagosomes in which podosomes were disrupted (neighbor image). Interestingly, only cells that ingested particles lost transiently their podosomes, neighbor cells without phagosomes kept their podosomes (Fig. 2A, right panels). Podosome quantification was performed. It showed that phagocytosis of IgG-LB induced a loss of podosomes in 70 % of the cells with phagosomes at 15 min and then the number of cells with podosomes raised back to normal at 60 min (Fig. 2). In contrast, phagocytosis of LB was not associated with podosome loss over the 3 h time-course of the experiments (Fig. 2). When phagocytosis was performed with zymosan (Z) and OZ used at 30 and 10 particles/cells respectively to keep comparable phagocytosis rates than latex beads (Suppl. Fig. 2A), transient podosome disappearance was observed with both types of particles (Suppl. Fig. 2B). Similarly to IgG-LB, only cells with phagosomes had transient podosome disruption (Suppl. Fig. 2B).

Next, the podosome number was quantified by cell surface unit in cells with phagosomes containing IgG-LB. After 5 min, the podosome number rapidly dropped down from 264 to 96 podosomes / 1000 μm^2 and went back to control at 60 min (270 podosomes /1000 μm^2) (Fig. 2C). We also quantified podosomes per cell surface unit in cells that ingested LB and no change was noticed (Fig. 2C). During phagocytosis of IgG-LB, the cell area of macrophages was reduced concomitantly to podosome disruption. When podosomes re-appeared, macrophage spreading increased without reaching the control value (Fig. 2).

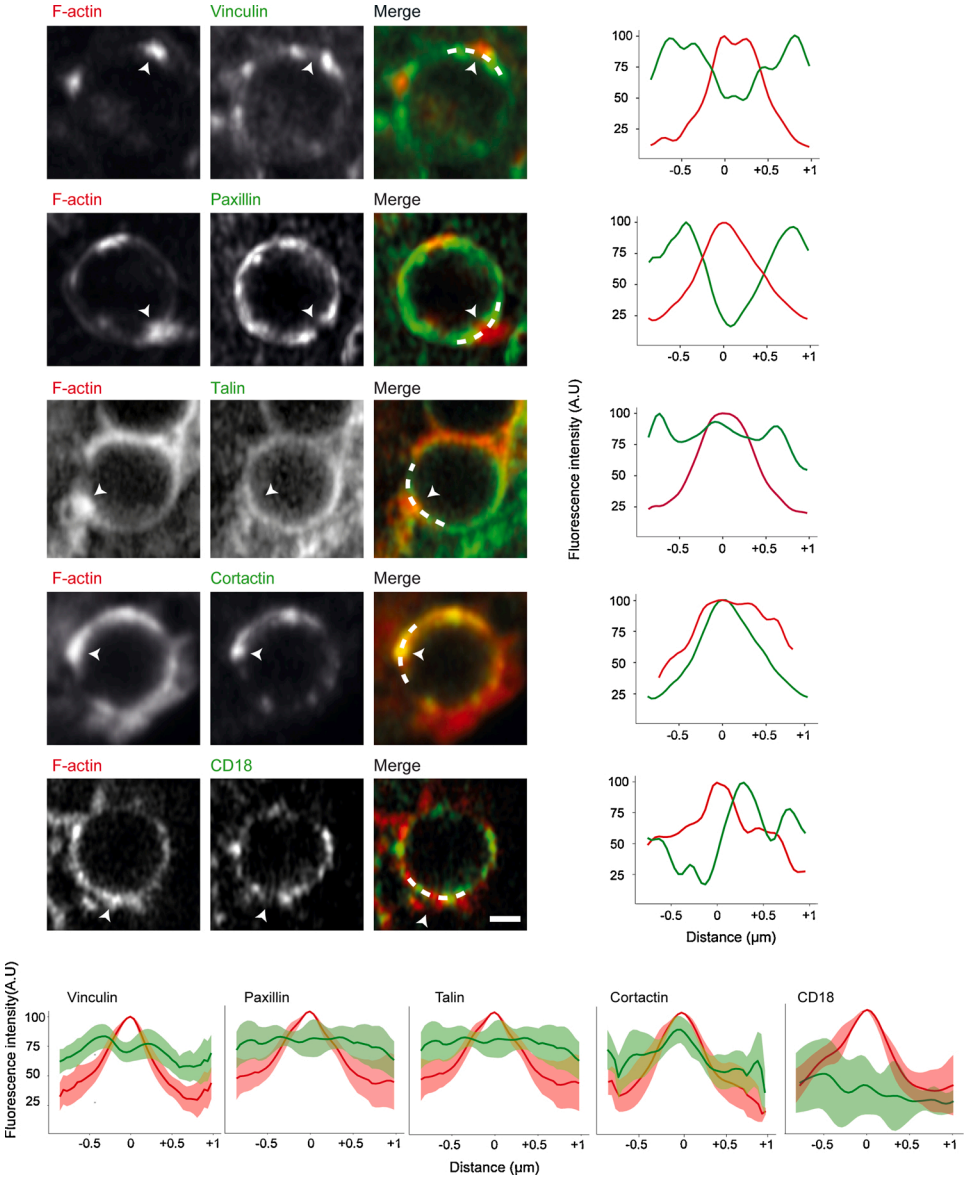

Fig. 3. F-actin structures present on closed phagosomes have podosome characteristics. Macrophages were exposed to IgG-LB for 10 min and F-actin (red), vinculin, paxillin, talin and cortactin were stained (green) or for 5 min and F-actin and CD18 were stained. Super-resolution images show phagosomes (scale bar : 1 µm) used for the line scans (right) with zero on the horizontal axis corresponding to the center of PAPs. Line scan mean values were calculated from at least 10 PAPs from 3 donors, using PlotTwist application (lower panels). (For interpretation of the references to colour in this figure legend, the reader is referred to the web version of this article).

However, this transient decrease of the cell spreading also occurred in cells ingesting LB that do not lose their podosomes suggesting that the two events are not correlated.

These experiments revealed that upon phagocytosis of most but not all phagocytic particles, those that trigger formation of actin structures at phagosomes also trigger transient podosome disruption. This occured exclusively in cells with phagosomes suggesting that a coupling exists between phagocytosis, formation of actin structures at phagosomes and podosome disruption.

3.3. *F-actin structures present on closed phagosomes have podosome characteristics*

The actin structures present on closed phagosomes were characterized to determine whether they share common features with podosome-like structures that were already described in phagocytic cups. Using confocal and super-resolution fluorescence microscopy, the height of F-actin foci on phagosomes was estimated to be 511 +/-107 nm (mean +/-SD of 16 actin foci from 7 cells, from 2 donors). We observed that podosome components belonging to the adhesion complex (integrins, vinculin, paxillin, talin) that are present in the ring of podosomes, also localized in close proximity of actin foci on phagosomes (Fig. 3). Analysis of fluorescence intensity profiles revealed that, similarly to podosomes, cortactin co-localized with F-actin and vinculin, paxillin and talin accumulated around the peak of F-actin (Fig. 3, Video 2). The αMβ2 integrin (CD18/CD11b) is involved in both adhesion complexes and FcγR-mediated phagocytosis (Graham et al., 1989; Jongstra-Bilen et al., 2003). We observed that 91.7 ± 18.5 %, n = 2 of

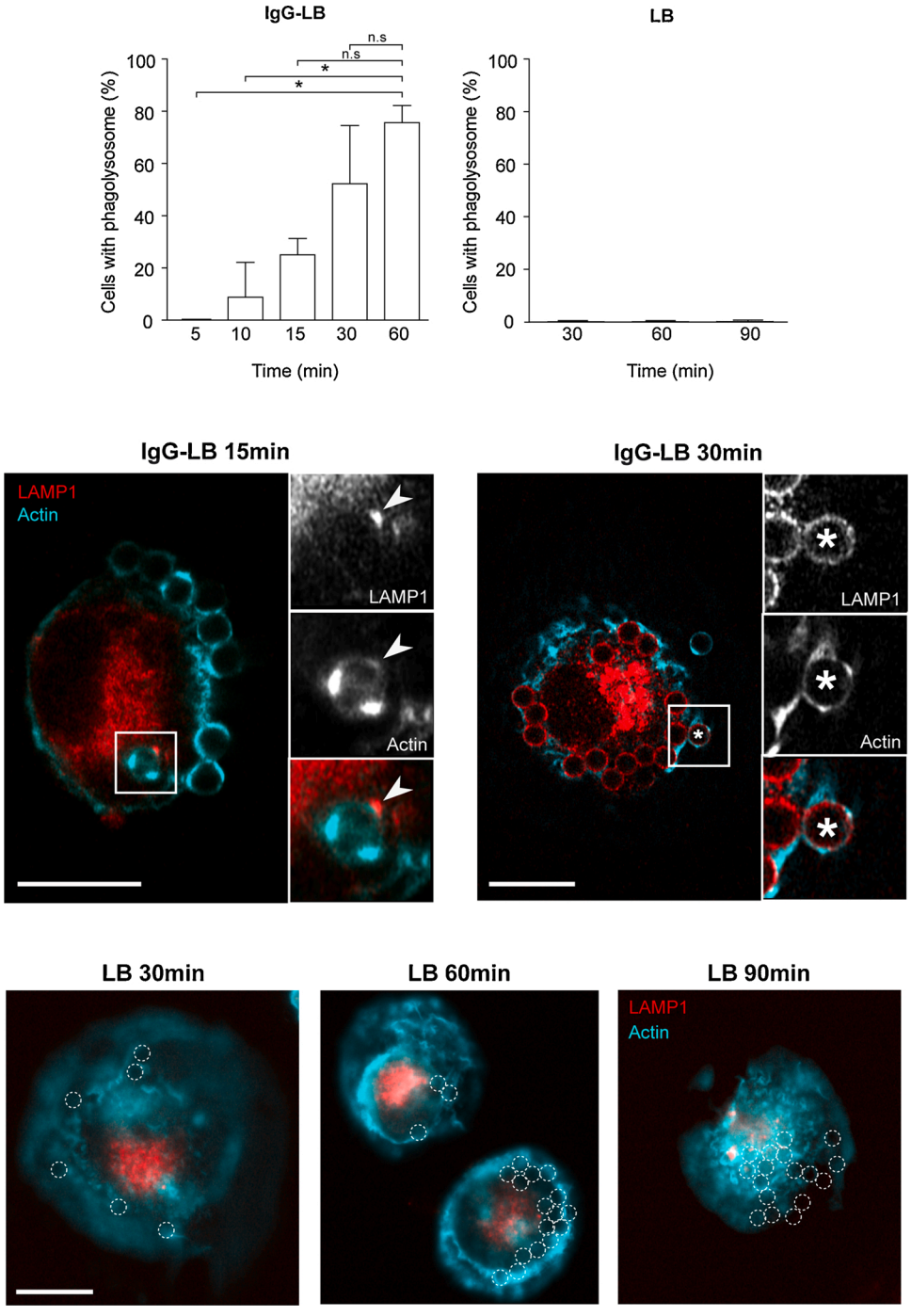

Fig. 4. Differential phagolysosome formation upon ingestion of IgG-LB or LB by human macrophages. Upper panels: Phagolysosomes (Lamp-1 positive) were quantified at different time points in cells challenged with IgG-LB or LB. The results are expressed as mean +/- SD, n = 3 and analyzed using Kruskal-Wallis test, followed by Dunn's multiple comparisons test. Middle panels: representative superresolution microscopy images of macrophages exposed to IgG-LB stained for LAMP-1 (red) and F-actin (cyan) at 15 and 35 min. The arrowheads show a LAMP-1 positive vesicle in proximity of a phagosome with PAPs. The stars show a phagosome with both LAMP-1 and PAPs at its membrane. Lower panels : Fluorescence microscopy images of F-actin and LAMP-1 are not recruited to phagosomes containing LB (represented by dash circles) at different time points. (For interpretation of the references to colour in this figure legend, the reader is referred to the web version of this article).

actin-positive phagosomes were also CD18 positive. Analysis of the fluorescence intensity profiles revealed that CD18 was present in close proximity of F-actin foci (Fig. 3).

Next, the life-time of these phagosome-associated F-actin structures was determined by confocal microscopy in macrophages transduced with LifeAct-mCherry. F-actin was monitored for an hour in single cells (Video 3) that perform phagocytosis of IgG-LB in a non-synchronized way. We found that the mean life-span of F-actin foci on phagosomes was 5.0 +/- 3.3 min (Suppl. Fig. 3). In the meantime, podosomes progressively disappeared from the ventral face of macrophages (Video 3).

Thus, podosomes and F-actin foci at phagosomes share common characteristics: similar size since podosomes are structured as an actin core of 5−600 nm high surrounded by a ring of adhesion proteins of 0.8−1 µm (Labernadie et al., 2010; Wiesner et al., 2010); similar life span; similar protein components (integrin, talin, vinculin, paxillin, cortactin) with similar localizations to podosomes. We therefore propose to call these F-actin structures phagosome-associated podosomes (PAPs).

3.4. The presence of PAPs correlates with phagolysosome formation

Podosomes are docking sites for intracellular vesicles that subsequently fuse with the membrane and deliver metalloproteases and cathepsins involved in extracellular matrix degradation (Cougoule et al., 2005; Jevnikar et al., 2012; Van Goethem et al., 2010; Wiesner et al., 2010). Hence we wondered whether PAPs would display similar functionality, since phagosomes fuse with endosomes and lysosomes to form phagolysosomes along the maturation process.

The formation of phagolysosomes was examined by monitoring the transfer of lysosome-associated membrane protein 1 (LAMP-1) to the membrane of phagosomes. During phagocytosis of IgG-LB by human macrophages, LAMP-1 positive phagosomes were detected from 10 min on (Fig. 4). As shown in Fig. 4 (15 min, arrowhead), a LAMP-1-positive vesicle was in close proximity to an IgG-LB phagosome with PAPs. In Fig. 4 (30 min, star) a phagosome with both PAPs and LAMP-1 is shown. When this phenomenon was quantified, only 15+/-6% (n = 3 donors) of phagosomes were F-actin and LAMP-1 double positive suggesting that PAPs rapidly disappeared after LAMP-1 transfer. Supporting this, PAPs decreased with time (Fig. 1B left graph) while phagolysosomes increased (Fig. 4, left graph).

In contrast to IgG-LB, phagosomes containing LB did not become LAMP-1 positive at any time point examined until 90 min (Fig. 4).

These results suggest that phagocytic particles that do not trigger the formation of PAPs do not end up in phagolysosomes.

3.5. Formation of PAPs involves integrins and is resistant to Arp2/3 inhibition

CD11b/CD18 is involved in phagocytosis of IgG, it accumulates at phagocytic cups and podosome-like structures (Graham et al., 1989; Jongstra-Bilen et al., 2003; Freeman et al., 2016; Ostrowski et al., 2019). When integrins were inhibited with EDTA which chelates divalent cations (Zhang and Chen, 2012), we observed that the percentage of phagosomes with PAPs was decreased, suggesting that integrin activation was involved, at least for a part, in PAPs formation (Fig. 5A).

The formation of podosomes is Arp2/3-dependent (Faust et al., 2019; Jeannot and Besson, 2020; van den Dries et al., 2019; Yamaguchi et al., 2005), and the formation of actin flashes at the phagosomal membrane as well (Poirier et al., 2020). Thus we questioned the involvement of Arp2/3 in the formation of PAPs. Recently, the role of Arp2/3 in the process of phagocytosis has been re-evaluated (Rotty et al., 2017). Indeed, macrophages from Arp2c-/- mice or macrophages treated with the Arp2/3 inhibitor CK666 are still capable of ingesting IgG-coated particles. So, we compared the effect of CK666 (Baggett et al., 2012) on podosomes, PAPs and phagolysosome formation in macrophages ingesting IgG-LB. We first determined the lowest concentration of CK666 sufficient to abolish the formation of podosomes without major effect on phagocytosis of IgG-LB. Using 50 µM CK666, podosomes were almost fully disrupted while phagocytosis of IgG-LB, formation of PAPs and LAMP-1 translocation to the phagosomal membrane were not significantly modified (Fig. 5B-C). In other studies, CK666 has been used at 150 µM to inhibit the formation of F-actin flashes on phagosomes (Poirier et al., 2020) or phagocytosis of C3bi-coated particles by macrophages (Rotty et al., 2017). Thus, we examined whether higher concentrations of CK666 would affect PAPs. Using CK666 at 100 and 150 µM we observed that podosomes were completely disrupted (Fig. 5D), phagocytosis of IgG-LB was slightly inhibited (21 % with 150µM CK666 at 30 min), and the percentage of phagosomes with PAPs was decreased but not significantly (Fig. 5E). In the presence of 150 µM CK666, cortactin which is known as a regulator of Arp2/3 (Kirkbride et al., 2011)

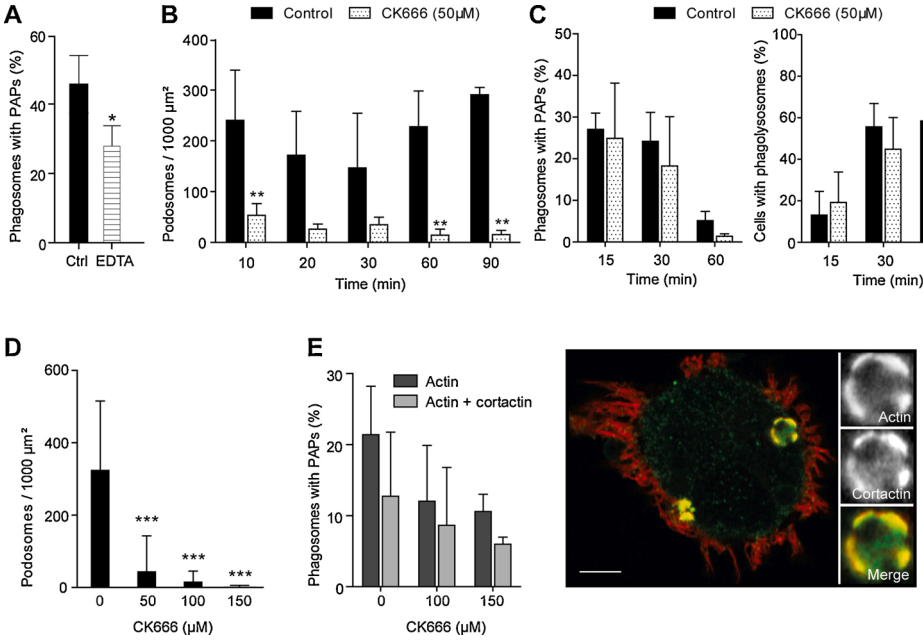

Fig. 5. Arp2/3 inhibition disrupts podosomes but PAPs and phagolysosomes are only slightly affected. (A) EDTA (5 mM) inhibited the formation of PAPs on IgG-LB containing phagosomes. Data from at least 180 cells from 6 donors are expressed as mean +/- SD and analyzed using paired *t*-test followed by Wilcoxon test. (B-C) The podosome density was markedly decreased by 50 µM CK666; PAPs persisted on IgG-phagosomes and phagolysosome formation was not affected by CK666. Data from at least 50 cells from 3 donors are expressed as mean +/- SD and analyzed using two-way ANOVA followed by Bonferroni's multiple comparison test. (D) High concentrations of CK666 abolished the formation of podosomes. (E) The localization of cortactin was not modified by 150 µM CK666 in macrophages ingesting IgG-LB for 30 min, a merge Airyscan microscopy image shows that cortactin (green) co-localized with F-actin (red) in PAPs. Scale bar 5 µm. For D and E : data from at least 70 cells from 3 donors are expressed as mean +/- SD and were analyzed using Kruskal-Wallis test. (For interpretation of the references to colour in this figure legend, the reader is referred to the web version of this article).

still co-localized with the actin core of PAPs, like it does in untreated cells (Fig. 5E). Thus, even at high CK666 concentration, PAPs are still present and organized like in controls. These results indicate that PAPs, like podosomes, involve integrin activation but they can be distinguished from podosomes by being partially resistant to Arp2/3 inhibition by CK666.

4. Discussion

Actin polymerization at nascent phagosomes has been studied with interest in order to understand how pseudopodia progress around the particle, how the membrane adheres to the particle and senses its stiffness (Jaumouille and Waterman, 2020; Liebl and Griffiths, 2009; Ostrowski et al., 2019). There are podosomes-like structures on phagocytic cups (Allen and Aderem, 1996; Labrousse et al., 2011; Ostrowski et al., 2019) and, actin flashes on closed phagosomes (Liebl and Griffiths, 2009; Poirier et al., 2020). These two structures can be distinguished by several aspects including their size, life span, duration and the phagocytic receptors involved (Liebl and Griffiths, 2009; Ostrowski et al., 2019; Poirier et al., 2020).

Here, we describe actin structures that form on both phagocytic cups and closed phagosomes containing various particle types. They have structural characteristics of podosomes, and, similarly to podosomes that are targeted by vesicles, they are involved in phagosome maturation into phagolysosomes. We called these actin structures phagosome-associated podosomes (PAPs). Concomitant to PAP formation, podosomes transiently disappeared in macrophages containing phagosomes, not in cell neighbors devoid of phagosomes suggesting that PAPs form at the expense of podosomes.

We noticed that PAPs did not form when LB were ingested, whereas they appeared on IgG-LB phagosomes. Depending on the concerned particle, phagocytosis involves the complex interplay of receptors for serum opsonins, microbes or senescent cell motifs that initiate a diversity of signaling pathways. In the case of LB, CD36 and P2×7 scavenger receptors have been proposed to participate in their internalization, but the signals they elicit during that process have not been identified (Wiley and Gu, 2012; Yun et al., 2014). The receptors of OZ, zymosan and IgG-LB have been better characterized. OZ is recognized by several receptors which bind to IgG (FcγRs) and by the integrin αMβ2, also called Complement Receptor 3 (CR3), which binds to the complement fragment C3bi. Receptors for zymosan include the mannose receptor, dectin1 and the lectin domain of the CR3 (Astarie-Dequeker et al., 1999; Ganbold and Baigude, 2018; Le Cabec et al., 2002; Ross et al., 1985). The receptors involved in ingestion of IgG-LB are FcγRs and, interestingly, during phagocytosis of IgG, β2 integrins and integrin-associated proteins have been described to accumulate on phagosomes (Allen and Aderem, 1996; Freeman et al., 2016; Greenberg et al., 1990; Jaumouille and Grinstein, 2016; Labrousse et al., 2011). More specifically, in the context of IgG-mediated frustrated phagocytosis, activated β2 integrins accumulate in the environment of podosome-like structures (Ostrowski et al., 2019) and, during phagocytosis of IgG-LB, β2 integrins were observed on phagosomes in close proximity with PAPs (this report). It is well established that integrins and FcγRs trigger actin polymerization but it is not known whether the receptors involved in phagocytosis of LB induce actin polymerization which was only occasionally observed on LB phagosomes.

Another difference between the particles we used, is the process of phagosome maturation. Once phagosomes are closed, approximately 5 min after the beginning of particle engulfment, they migrate towards the cell center and maturate by sequential fusion with vesicles of the endosome-lysosome compartments to form phagolysosomes. In a few examples however, ingested cargos are not routed to phagolysosomes (Armstrong and Hart, 1971). In the case of phagosomes containing LB, most of them (>95 %, n = 4) remained negative for both the early endosome protein Rab5 and the late endosome/lysosome protein LAMP-1 (this report), and were previously shown to by-pass the production of O_2^-, a major bactericidal response of human macrophages (Astarie-Dequeker et al., 1999). This is different from phagosomes containing LB previously shown to become Rab 5 and LAMP-1 positive in the J774 cell line (Houde et al., 2003). However, several differences between human primary macrophages and this particular mouse macrophage-like cell line isolated from a murine sarcoma have been reported (Andreu et al., 2017; Chamberlain et al., 2015; Hall et al., 2006), so we assume that phagosome maturation proceeds differently in these two cell types. Contrasting with LB, phagosomes containing IgG-LB, Z and OZ formed PAPs and became LAMP-1 positive (this report). These observations allowed to propose that the presence of PAPs is related to late endosome/lysosome fusion. Dense actin meshworks that make a physical barrier around early phagosomes impair their fusion with vesicles (Burgoyne and Cheek, 1987; Liebl and Griffiths, 2009), and progressively disappear during phagosome maturation. However, F-actin is still assembling at discrete sites of the phagosome membrane, a process required for fusion of late endosomes/lysosomes with phagosomes (Anes et al., 2003; Hasegawa et al., 2016; Kalamidas et al., 2006; Kjeken et al., 2004; Liebl and Griffiths, 2009; Marion et al., 2011; Wang et al., 2008). Thus, in the light of these observations, we propose that PAPs on closed phagosomes could be the F-actin structures that serve as docking sites for vesicles. In fact, in the vicinity of PAPs, LAMP1-positive vesicles were observed. However, phagosomes were more frequently PAPs positive or LAMP-1 positive rather than double-positive suggesting that co-existence of both staining should be a short-lasting event. Similarly, in RAW264.7 macrophages, phagosomes containing IgG-LB have been shown to lose actin at their surface while acquiring LAMP-2 (Liebl and Griffiths, 2009). Thus, PAPs could serve as furtive docking and fusion sites for vesicles and subsequently disappear.

Like podosomes that are involved in cell adhesion, generation of protrusive forces, mechano- and topography-sensing, proteolysis of the extracellular matrix and cell migration, we propose that PAPs could be also multifunctional structures. Actually podosome-like structures on phagocytic cups have been described to seal the membrane to the phagocytic prey suggesting that the protrusion force generated by podosomes to sense the environment (Bouissou et al., 2017; Labernadie et al., 2014; van den Dries et al., 2019) is also operating in podosome-like structures to seal the membrane onto the ingested particle and, possibly, sense its stiffness (Ostrowski et al., 2019). Whether mechanosensing property is also functional in PAPs remains to be demonstrated, but the presence of proteins belonging to the adhesion complex spatially organized like in podosomes and podosome-like structures on frustrated phagosomes is in favor of this hypothesis. The Arp2/3 complex is a major regulator of actin filament assembly involved in podosome formation. Here, we show that PAPs are poorly disturbed by the presence of 150 μM CK666, a concentration that abolished the formation of podosomes in the same cells (this report), the formation of actin flashes (Poirier et al., 2020) and phagocytosis of C3bi coated beads (Rotty et al., 2017). Similarly to PAPs formation, phagocytosis of IgG particles, triggers an Arp2/3-independent route to actin polymerization which compensates for Arp2/3 inhibition (Rotty et al., 2017). Formins are actin nucleators which function independently of Arp2/3. They generate unbranched actin filaments. The formin family comprises 15 proteins, several of them have been implicated in the formation of podosomes and invadopodia, and degradation of the extracellular matrix (Lizarraga et al., 2009; Mersich et al., 2010; Miller et al., 2017; Panzer et al., 2016; Ren et al., 2018; Tsuboi et al., 2009). Thus we propose that formins could complement Arp2/3 in the formation of PAPs, explaining their pretty good resistance to Arp2/3 inhibition. Actually, in addition to its role in Arp2/3 activation, cortactin which co-localized with F-actin in PAPs has been described to recruit formins in invadopodia (Li et al., 2010; Ren et al., 2018; Suman et al., 2018). To explore whether formins could be involved in actin polymerization in PAPs, 25 μM SMIFH2, a formin pan-inhibitor (Isogai et al., 2015) was used but it did not affect PAP formation (data not shown), pointing to the need of more specific approaches.

So, podosome-like structures and PAPs share many structural and functional characteristics with podosomes but differ by a few aspects. In the case of podosome-like structures, inhibition of two PI(3,4,5)P3 effectors Akt and ARNO required for podosomes formation have no obvious effect (Ostrowski et al., 2019). In the case of PAPs, inhibition of Arp2/3 has almost undetectable effect whereas, in the same cells, podosomes are completely dismantled. It is possible that the structural differences have consequences on the functions deserved by podosomes-like structures and PAPs at the phagosomal membrane compared to podosomes at the interface between the plasma membrane and the substratum. In addition to podosomes at phagosomes, other "unusual localizations" of podosomes have been reported including at cell interfaces during cell-cell fusion and at the immunological synapse (Faust et al., 2019; Oikawa et al., 2012; Wernimont et al., 2008). Whether podosomes in these localizations also present some signaling, structural and functional differences from "classical" podosomes has not been explored and this opens a new research field.

In this study, we also show that podosomes were temporarily dismantled concomitantly to the formation of PAPs. Strikingly, it occurred during ingestion of IgG-opsonized particles, zymosan and serum-opsonized zymosan, but not that of LB. PAPs were present at 5 min, the earliest time point of our experiments and disappeared about 60 min later. Podosomes disappeared and reappeared with almost the same kinetics. Transient disruption of podosomes was only observed in cells that had ingested particles, podosomes remained unaffected in neighboring cells that lacked phagosomes. It indicates that the process of phagocytosis by itself is involved in a way that is not triggered by LB. One hypothesis is that the signaling of phagocytic receptors involved in ingestion of IgG-LB, Z and OZ triggers podosome disruption. A molecule which spreads from a cell to another such as PGE2, known to disrupt podosomes in dendritic cells (Cougoule et al., 2018; van Helden et al., 2008), can be excluded because macrophages without phagosomes keep their podosomes. Podosomes and PAPs share adhesion complexes containing talin, paxillin and vinculin that link integrins to actin. Several actors regulating this process such as FAK/Pyk2 and Src kinases could be potential limiting factors. As a consequence, their recruitment on forming phagosomes to initiate the ingestion process and form PAPs would deplete them at the ventral face of macrophages, which could induce podosome disruption. Interestingly, podosome disruption would be potentially a way to redirect lysosomes to PAPs and no longer to podosomes, and thus prioritize the destruction of phagocytic particles at the expense of podosome-mediated matrix degradation.

To conclude, we propose that PAPs and podosome-like structures described in phagocytic cups are similar structures, themselves related to podosomes. Formation of PAPs leads to phagosome maturation and to podosome disruption in a synchronized manner. The rationality to disrupt podosomes when PAPs are present is not understood yet, it could help at redirecting vesicles containing proteases to phagosomes to digest microorganisms, which is undoubtedly a life priority.

Fundings

This work was supported by the Human Frontier Science Program (RGP0035/2016), Fondation pour la Recherche MedicaleDEQ2016 0334894RGP0035/2016, Inserm Plan Cancer, Fondation Toulouse Cancer Santé. CB is a recipient of a CNRS 80 Prime fellowship.

Declaration of Competing Interest

The authors have no competing interests to declare.

Acknowledgements

The authors thank TRI imaging facility, Veronique Le Cabec for critical reading of the manuscript, Christel Verollet and Remi Mascarau for helpful discussions.

Appendix A. Supplementary data

Supplementary material related to this article can be found, in the online version, at doi:https://doi.org/10.1016/j.ejcb.2021.151161.

References

Allen, L.A., Aderem, A., 1996. Molecular definition of distinct cytoskeletal structures involved in complement- and Fc receptor-mediated phagocytosis in macrophages. J. Exp. Med. 184, 627–637.
Andreu, N., Phelan, J., de Sessions, P.F., Cliff, J.M., Clark, T.G., Hibberd, M.L., 2017. Primary macrophages and J774 cells respond differently to infection with Mycobacterium tuberculosis. Sci. Rep. 7, 42225.
Anes, E., Kuhnel, M.P., Bos, E., Moniz-Pereira, J., Habermann, A., Griffiths, G., 2003. Selected lipids activate phagosome actin assembly and maturation resulting in killing of pathogenic mycobacteria. Nat. Cell Biol. 5, 793–802.
Armstrong, J.A., Hart, P.D., 1971. Response of cultured macrophages to Mycobacterium tuberculosis, with observations on fusion of lysosomes with phagosomes. J. Exp. Med. 134, 713–740.
Astarie-Dequeker, C., N'Diaye, E.N., Le Cabec, V., Rittig, M.G., Prandi, J., Maridonneau-Parini, I., 1999. The mannose receptor mediates uptake of pathogenic and nonpathogenic mycobacteria and bypasses bactericidal responses in human macrophages. Infect. Immun. 67, 469–477.
Baggett, A.W., Cournia, Z., Han, M.S., Patargias, G., Glass, A.C., Liu, S.Y., Nolen, B.J., 2012. Structural characterization and computer-aided optimization of a small-molecule inhibitor of the Arp2/3 complex, a key regulator of the actin cytoskeleton. ChemMedChem 7, 1286–1294.
Bouissou, A., Proag, A., Bourg, N., Pingris, K., Cabriel, C., Balor, S., Mangeat, T., Thibault, C., Vieu, C., Dupuis, G., Fort, E., Leveque-Fort, S., Maridonneau-Parini, I., Poincloux, R., 2017. Podosome force generation machinery: a local balance between protrusion at the core and traction at the ring. ACS Nano 11, 4028–4040.
Burgoyne, R.D., Cheek, T.R., 1987. Reorganisation of peripheral actin filaments as a prelude to exocytosis. Biosci. Rep. 7, 281–288.
Caron, E., Hall, A., 1998. Identification of two distinct mechanisms of phagocytosis controlled by different Rho GTPases. Science 282, 1717–1721.
Chamberlain, L.M., Holt-Casper, D., Gonzalez-Juarrero, M., Grainger, D.W., 2015. Extended culture of macrophages from different sources and maturation results in a common M2 phenotype. J. Biomed. Mater. Res. A. 103, 2864–2874.
Cougoule, C., Carreno, S., Castandet, J., Labrousse, A., Astarie-Dequeker, C., Poincloux, R., Le Cabec, V., Maridonneau-Parini, I., 2005. Activation of the lysosome-associated p61Hck isoform triggers the biogenesis of podosomes. Traffic 6, 682–694.
Cougoule, C., Le Cabec, V., Poincloux, R., Al Saati, T., Mege, J.L., Tabouret, G., Lowell, C. A., Laviolette-Malirat, N., Maridonneau-Parini, I., 2010. Three-dimensional migration of macrophages requires Hck for podosome organization and extracellular matrix proteolysis. Blood 115 (7), 1444–1452.
Cougoule, C., Lastrucci, C., Guiet, R., Mascarau, R., Meunier, E., Lugo-Villarino, G., Neyrolles, O., Poincloux, R., Maridonneau-Parini, I., 2018. Podosomes, but not the maturation status, determine the protease-dependent 3D migration in human dendritic cells. Front. Immunol. 9, 846.
Faust, J.J., Balabiyev, A., Heddleston, J.M., Podolnikova, N.P., Baluch, D.P., Chew, T.L., Ugarova, T.P., 2019. An actin-based protrusion originating from a podosome-enriched region initiates macrophage fusion. Mol. Biol. Cell 30, 2254–2267.
Freeman, S.A., Grinstein, S., 2014. Phagocytosis: receptors, signal integration, and the cytoskeleton. Immunol. Rev. 262, 193–215.
Freeman, S.A., Goyette, J., Furuya, W., Woods, E.C., Bertozzi, C.R., Bergmeier, W., Hinz, B., van der Merwe, P.A., Das, R., Grinstein, S., 2016. Integrins form an expanding diffusional barrier that coordinates phagocytosis. Cell 164, 128–140.
Ganbold, T., Baigude, H., 2018. Design of mannose-functionalized curdlan nanoparticles for macrophage-targeted siRNA delivery. ACS Appl. Mater. Interfaces 10, 14463–14474.
Goedhart, J., 2020. PlotTwist: a web app for plotting and annotating continuous data. PLoS Biol. 18, e3000581.
Graham, I.L., Gresham, H.D., Brown, E.J., 1989. An immobile subset of plasma membrane CD11b/CD18 (Mac-1) is involved in phagocytosis of targets recognized by multiple receptors. J. Immunol. 142, 2352–2358.
Gray, M., Botelho, R.J., 2017. Phagocytosis: hungry, hungry cells. Methods Mol. Biol. 1519, 1–16.
Greenberg, S., Burridge, K., Silverstein, S.C., 1990. Colocalization of F-actin and talin during Fc receptor-mediated phagocytosis in mouse macrophages. J. Exp. Med. 172, 1853–1856.
Hall, A.B., Gakidis, M.A., Glogauer, M., Wilsbacher, J.L., Gao, S., Swat, W., Brugge, J., 2006. Requirements for Vav guanine nucleotide exchange factors and Rho GTPases in FcgammaR- and complement-mediated phagocytosis. Immunity. 24, 305–316.
Hasegawa, J., Iwamoto, R., Otomo, T., Nezu, A., Hamasaki, M., Yoshimori, T., 2016. Autophagosome-lysosome fusion in neurons requires INPP5E, a protein associated with Joubert syndrome. EMBO J. 35, 1853–1867.
Houde, M., Bertholet, S., Gagnon, E., Brunet, S., Goyette, G., Laplante, A., Princiotta, M. F., Thibault, P., Sacks, D., Desjardins, M., 2003. Phagosomes are competent organelles for antigen cross-presentation. Nature. 425, 402–406.
Isogai, T., van der Kammen, R., Innocenti, M., 2015. SMIFH2 has effects on Formins and p53 that perturb the cell cytoskeleton. Sci. Rep. 5, 9802.

Jahraus, A., Egeberg, M., Hinner, B., Habermann, A., Sackman, E., Pralle, A., Faulstich, H., Rybin, V., Defacque, H., Griffiths, G., 2001. ATP-dependent membrane assembly of F-actin facilitates membrane fusion. Mol. Biol. Cell 12, 155–170.
Jakubzick, C.V., Randolph, G.J., Henson, P.M., 2017. Monocyte differentiation and antigen-presenting functions. Nat. Rev. Immunol. 17, 349–362.
Jaumouille, V., Grinstein, S., 2016. Molecular mechanisms of phagosome formation. Microbiol. Spectr. 4.
Jaumouille, V., Waterman, C.M., 2020. Physical constraints and forces involved in phagocytosis. Front. Immunol. 11, 1097.
Jeannot, P., Besson, A., 2020. Cortactin function in invadopodia. Small GTPases 11, 256–270.
Jevnikar, Z., Mirkovic, B., Fonovic, U.P., Zidar, N., Svajger, U., Kos, J., 2012. Three-dimensional invasion of macrophages is mediated by cysteine cathepsins in protrusive podosomes. Eur. J. Immunol. 42, 3429–3441.
Jongstra-Bilen, J., Harrison, R., Grinstein, S., 2003. Fcgamma-receptors induce Mac-1 (CD11b/CD18) mobilization and accumulation in the phagocytic cup for optimal phagocytosis. J. Biol. Chem. 278, 45720–45729.
Kalamidas, S.A., Kuehnel, M.P., Peyron, P., Rybin, V., Rauch, S., Kotoulas, O.B., Houslay, M., Hemmings, B.A., Gutierrez, M.G., Anes, E., Griffiths, G., 2006. cAMP synthesis and degradation by phagosomes regulate actin assembly and fusion events: consequences for mycobacteria. J. Cell. Sci. 119, 3686–3694.
Kirkbride, K.C., Sung, B.H., Sinha, S., Weaver, A.M., 2011. Cortactin: a multifunctional regulator of cellular invasiveness. Cell Adh. Migr. 5, 187–198.
Kjeken, R., Egeberg, M., Habermann, A., Kuehnel, M., Peyron, P., Floetenmeyer, M., Walther, P., Jahraus, A., Defacque, H., Kuznetsov, S.A., Griffiths, G., 2004. Fusion between phagosomes, early and late endosomes: a role for actin in fusion between late, but not early endocytic organelles. Mol. Biol. Cell 15, 345–358.
Labernadie, A., Thibault, C., Vieu, C., Maridonneau-Parini, I., Charriere, G.M., 2010. Dynamics of podosome stiffness revealed by atomic force microscopy. Proc. Natl. Acad. Sci. U. S. A. 107, 21016–21021.
Labernadie, A., Bouissou, A., Delobelle, P., Balor, S., Voituriez, R., Proag, A., Fourquaux, I., Thibault, C., Vieu, C., Poincloux, R., Charriere, G.M., Maridonneau-Parini, I., 2014. Protrusion force microscopy reveals oscillatory force generation and mechanosensing activity of human macrophage podosomes. Nat. Commun. 5, 5343.
Labrousse, A., Record, J., Labernadie, A., Beduer, A., Vieu, C., Ben Safta, T., Maridonneau-Parini, I., 2011. Frustrated phagocytosis on micro-patterned immune complexes to characterize lysosome movements in live macrophages. Front. Immun. 2, 51. https://doi.org/10.3389/fimmu.2011.00051.
Le Cabec, V., Carreno, S., Moisand, A., Bordier, C., Maridonneau-Parini, I., 2002. Complement receptor 3 (CD11b/CD18) mediates type I and type II phagocytosis during nonopsonic and opsonic phagocytosis, respectively. J. Immunol. 169, 2003–2009.
Li, A., Dawson, J.C., Forero-Vargas, M., Spence, H.J., Yu, X., Konig, I., Anderson, K., Machesky, L.M., 2010. The actin-bundling protein fascin stabilizes actin in invadopodia and potentiates protrusive invasion. Curr. Biol. 20, 339–345.
Liebl, D., Griffiths, G., 2009. Transient assembly of F-actin by phagosomes delays phagosome fusion with lysosomes in cargo-overloaded macrophages. J. Cell. Sci. 122, 2935–2945.
Lizarraga, F., Poincloux, R., Romao, M., Montagnac, G., Le Dez, G., Bonne, I., Rigaill, G., Raposo, G., Chavrier, P., 2009. Diaphanous-related formins are required for invadopodia formation and invasion of breast tumor cells. Cancer Res. 69, 2792–2800.
Marchesin, V., Castro-Castro, A., Lodillinsky, C., Castagnino, A., Cyrta, J., Bonsang-Kitzis, H., Fuhrmann, L., Irondelle, M., Infante, E., Montagnac, G., Reyal, F., Vincent-Salomon, A., Chavrier, P., 2015. ARF6-JIP3/4 regulate endosomal tubules for MT1-MMP exocytosis in cancer invasion. J. Cell Biol. 211, 339–358.
Maridonneau-Parini, I., 2014. Control of macrophage 3D migration: a therapeutic challenge to limit tissue infiltration. Immunol. Rev. 262, 216–231.
Marion, S., Hoffmann, E., Holzer, D., Le Clainche, C., Martin, M., Sachse, M., Ganeva, I., Mangeat, P., Griffiths, G., 2011. Ezrin promotes actin assembly at the phagosome membrane and regulates phago-lysosomal fusion. Traffic 12, 421–437.
Mersich, A.T., Miller, M.R., Chkourko, H., Blystone, S.D., 2010. The formin FRL1 (FMNL1) is an essential component of macrophage podosomes. Cytoskeleton Hoboken (Hoboken) 67, 573–585.
Miller, M.R., Miller, E.W., Blystone, S.D., 2017. Non-canonical activity of the podosomal formin FMNL1gamma supports immune cell migration. J. Cell. Sci. 130, 1730–1739.
Monteiro, P., Rosse, C., Castro-Castro, A., Irondelle, M., Lagoutte, E., Paul-Gilloteaux, P., Desnos, C., Formstecher, E., Darchen, F., Perrais, D., Gautreau, A., Hertzog, M., Chavrier, P., 2013. Endosomal WASH and exocyst complexes control exocytosis of MT1-MMP at invadopodia. J. Cell Biol. 203, 1063–1079.
Mylvaganam, S.M., Grinstein, S., Freeman, S.A., 2018. Picket-fences in the plasma membrane: functions in immune cells and phagocytosis. Semin. Immunopathol. 40, 605–615.
Oikawa, T., Oyama, M., Kozuka-Hata, H., Uehara, S., Udagawa, N., Saya, H., Matsuo, K., 2012. Tks5-dependent formation of circumferential podosomes/invadopodia mediates cell-cell fusion. J. Cell Biol. 197, 553–568.
Ostrowski, P.P., Freeman, S.A., Fairn, G., Grinstein, S., 2019. Dynamic podosome-like structures in nascent phagosomes are coordinated by phosphoinositides. Dev. Cell 50 (397–410), e393.
Panzer, L., Trube, L., Klose, M., Joosten, B., Slotman, J., Cambi, A., Linder, S., 2016. The formins FHOD1 and INF2 regulate inter- and intra-structural contractility of podosomes. J. Cell. Sci. 129, 298–313.
Poirier, M.B., Fiorino, C., Rajasekar, T.K., Harrison, R.E., 2020. F-actin flashes on phagosomes mechanically deform contents for efficient digestion in macrophages. J. Cell. Sci. 133.
Ren, X.L., Qiao, Y.D., Li, J.Y., Li, X.M., Zhang, D., Zhang, X.J., Zhu, X.H., Zhou, W.J., Shi, J., Wang, W., Liao, W.T., Ding, Y.Q., Liang, L., 2018. Cortactin recruits FMNL2 to promote actin polymerization and endosome motility in invadopodia formation. Cancer Lett. 419, 245–256.
Ross, G.D., Cain, J.A., Lachmann, P.J., 1985. Membrane complement receptor type three (CR3) has lectin-like properties analogous to bovine conglutinin as functions as a receptor for zymosan and rabbit erythrocytes as well as a receptor for iC3b. J. Immunol. 134, 3307–3315.
Rotty, J.D., Brighton, H.E., Craig, S.L., Asokan, S.B., Cheng, N., Ting, J.P., Bear, J.E., 2017. Arp2/3 complex is required for macrophage integrin functions but is dispensable for FcR phagocytosis and in vivo motility. Dev. Cell 42 (498–513), e496.
Suman, P., Mishra, S., Chander, H., 2018. High expression of FBP17 in invasive breast cancer cells promotes invadopodia formation. Med. Oncol. 35, 71.
Tsuboi, S., Takada, H., Hara, T., Mochizuki, N., Funyu, T., Saitoh, H., Terayama, Y., Yamaya, K., Ohyama, C., Nonoyama, S., Ochs, H.D., 2009. FBP17 mediates a common molecular step in the formation of podosomes and phagocytic cups in macrophages. J. Biol. Chem. 284, 8548–8556.
Uribe-Querol, E., Rosales, C., 2020. Phagocytosis: our current understanding of a universal biological process. Front. Immunol. 11, 1066.
van den Dries, K., Linder, S., Maridonneau-Parini, I., Poincloux, R., 2019. Probing the mechanical landscape - new insights into podosome architecture and mechanics. J. Cell. Sci. 132.
Van Goethem, E., Poincloux, R., Gauffre, F., Maridonneau-Parini, I., Le Cabec, V., 2010. Matrix architecture dictates three-dimensional migration modes of human macrophages: differential involvement of proteases and podosome-like structures. J. Immunol. 184, 1049–1061.
Van Goethem, E., Guiet, R., Balor, S., Charriere, G.M., Poincloux, R., Labrousse, A., Maridonneau-Parini, I., Le Cabec, V., 2011. Macrophage podosomes go 3D. Eur. J. Cell Biol. 90, 224–236.
van Helden, S.F., Oud, M.M., Joosten, B., Peterse, N., Figdor, C.G., van Leeuwen, F.N., 2008. PGE2-mediated podosome loss in dendritic cells is dependent on actomyosin contraction downstream of the RhoA-Rho-kinase axis. J. Cell. Sci. 121, 1096–1106.
Wang, Q.Q., Li, H., Oliver, T., Glogauer, M., Guo, J., He, Y.W., 2008. Integrin beta 1 regulates phagosome maturation in macrophages through Rac expression. J. Immunol. 180, 2419–2428.
Wernimont, S.A., Cortesio, C.L., Simonson, W.T., Huttenlocher, A., 2008. Adhesions ring: a structural comparison between podosomes and the immune synapse. Eur. J. Cell Biol. 87, 507–515.
Wiesner, C., Faix, J., Himmel, M., Bentzien, F., Linder, S., 2010. KIF5B and KIF3A/KIF3B kinesins drive MT1-MMP surface exposure, CD44 shedding, and extracellular matrix degradation in primary macrophages. Blood 116, 1559–1569.
Wiley, J.S., Gu, B.J., 2012. A new role for the P2X7 receptor: a scavenger receptor for bacteria and apoptotic cells in the absence of serum and extracellular ATP. Purinergic Signal. 8, 579–586.
Yam, P.T., Theriot, J.A., 2004. Repeated cycles of rapid actin assembly and disassembly on epithelial cell phagosomes. Mol. Biol. Cell 15, 5647–5658.
Yamaguchi, H., Lorenz, M., Kempiak, S., Sarmiento, C., Coniglio, S., Symons, M., Segall, J., Eddy, R., Miki, H., Takenawa, T., Condeelis, J., 2005. Molecular mechanisms of invadopodium formation: the role of the N-WASP-Arp2/3 complex pathway and cofilin. J. Cell Biol. 168, 441–452.
Yun, M.R., Seo, J.M., Park, H.Y., 2014. Visfatin contributes to the differentiation of monocytes into macrophages through the differential regulation of inflammatory cytokines in THP-1 cells. Cell. Signal. 26, 705–715.
Zhang, K., Chen, J., 2012. The regulation of integrin function by divalent cations. Cell Adh. Migr. 6, 20–29.